Int. J. Heat Mass Transfer. Vol. 34, No. 10, pp. 2483–2496, 1991
Printed in Great Britain

0017–9310/91 $3.00+0.00
Pergamon Press plc

Static flow instability onset in tubes, channels, annuli, and rod bundles

R. B. DUFFEY and E. D. HUGHES
Idaho National Engineering Laboratory, EG&G Idaho, Inc., Energy and Systems Technology, P.O. Box 1625, Idaho Falls, ID 83415, U.S.A.

(*Received* 1 *August* 1990 *and in final form* 5 *November* 1990)

Abstract—A theoretical model is developed for the onset of flow instability for vertical upflow and downflow of a boiling fluid in a constant pressure drop flow channel. The model is based on momentum and energy balance equations with an algebraic modeling of two-phase velocity-slip effects. Predictions of the theory are tested against experimental data for pressure, heat flux, length, inlet subcooling, and exit fluid quality effects. The predictions of the dependency of the minimum mass flux on these variables are in complete agreement with the trends of the data. The experimental data have been taken from round tube, rectangular channel, annuli, and rod bundle geometries, with vertical upflow and downflow, under both non-bulk boiling and net vapor generation conditions. The data collection given here appears to be among the most complete available in the literature. The theoretical results suggest a method for correlating about limited ranges of operating state parameters for a fixed geometry. The method is given in the paper along with specific correlating lines.

1. INTRODUCTION

In our earlier paper [1], we analyzed and predicted dryout at low flow conditions when local dry patches form. We now develop a completely new approach for steady two-phase flow stability, utilizing conventional formulations of the conservation laws. The method is based on defining the minimum in the pressure drop vs flow rate curve and leads to a general static instability law for both upflow and downflow.

Consider the flow in a heated tube or annulus of a two-phase or thermally expandable fluid, such as an air–water mixture or water alone with a constant pressure drop. The constant pressure drop boundary condition may be derived from the hydrostatic head of the loop or from a pump with one or more heated channels in parallel. At some condition, buoyancy or frictional forces will cause a reduction, oscillation, or even a reversal of the mean flow, which could then lead to wall dryout and temperature rise. To date, prediction of the onset of this condition is based on data, and is characterized experimentally by flow oscillation and an *increasing* pressure drop with *decreasing* flow rate [2]. The onset of the static instability or oscillation does not necessarily cause dryout, and is called an excursive flow or static instability, but often lies very close to the dryout point because the onset may be followed by limit cycle fluctuations in flow. Gambill and Bundy [3] refer to this as 'vapor binding' following flow oscillation preceding burnout. The practical interest lies in the determination of the limiting condition for safety control and/or operation, in parallel tube heat exchangers, boiling channels, boiling water reactors (BWRs), and natural circulation loops.

Much literature and data exist for the case of upflow, where manometer, dynamic (density) wave, and classic static Ledinegg (pressure drop) instability can occur (see, for example, refs. [4–10] and the references therein).† For downflow the obvious question is the applicability of the upflow work and the need for a predictive capability for static instability onset. The work of Whittle and Forgan [2] showed that downflow and upflow data for the flow rate at the minimum pressure drop point could be empirically correlated by a linear relation between the heat flux and flow rate, allowing for entry flow effects. Previous approaches have considered the linear perturbation or periodic numerical frequency domain solutions of the flow equations, taking these to represent the onset of dynamically unstable flow [3, 11, 12]. Methods utilizing transient (time-domain) solution of the flow equations for the heated channel have also been attempted [13, 14]. The results have been shown to be sensitive to the spatial discretization (nodalization) and numerical solution scheme adopted [15, 16]. No general correlation of a wide range of data exists, and comparisons of theories to data are generally very limited.

Other attempts to correlate the instability have centered on showing that the onset of nucleate boiling precedes the onset of unstable flow [17]. The Saha and Zuber [18] upflow correlation for the onset of subcooled nucleate boiling has been used for this pur-

† The Eindhoven Symposium on 'Two-phase Flow Dynamics", 1967, published as EUR-4288e in two volumes contains an excellent compendium of research results.

NOMENCLATURE

A	area
C	constant
D_e	equivalent diameter
f	friction factor
G	mass velocity
g	gravitational acceleration
h	enthalpy
Δh	enthalpy difference
j	superficial velocity
L	(test section) heated length
p	pressure
ΔP	pressure difference
ΔP^*	critical pressure ratio
q''	heat flux
S	slip ratio
t	time
u	velocity
X	quality
z	vertical ordinate.

Greek symbols

α	void fraction
ρ	density
$\Delta\rho$	density difference
Φ	two-phase friction multiplier.

Subscripts

d	departure
e	equilibrium
f	flow
fg	phase change
g	vapor
in	inlet
l	liquid
m	minimum
o	outlet
w	wall.

Dimensionless groups

N_{fg}	phase change number
N_s	subcooling number
L^*	instability number.

pose. We show that such agreement is not a sufficient condition (an observation with which Zuber agrees).† Indeed, comparisons by Saha *et al.* [9] for dynamic instability show this approach to be a lower bound only at very low subcoolings.

The important conclusions of the present work are that thermally expandable flows are inherently unstable; and that a simple correlation of existing data and new predictions can be made, which unifies downflow with the upflow case. We show the form of the Whittle and Forgan [2] correlation is theoretically justified, although the physical interpretation is quite different. The model equation derived in this work is entirely consistent with the trends observed in the experimental data for a wide range of pressures for flow in channels, tubes, annuli, and large rod bundles.

For completeness, we note that the physical phenomena that are omitted in the present model include the effects of void at bulk-subcooled thermodynamic states, variation of the two-phase friction multiplier with mass flux and vapor flow fraction, and the contribution of momentum flux to the stability criteria. It might at first be thought these simplifications severely limit the model; we use the scientific method, test the hypotheses, and show by comparisons, to data, that they are acceptable.

These omitted phenomena can and will be included into refined models as sufficiently detailed experimental data become available. Although these effects are not included in the present analysis, the results are in accord with all the available experimental data, within the data uncertainties, and cover wide ranges of channel geometry and operating conditions.

† Private communication with N. Zuber, Washington, DC, 1989.

2. THEORY

2.1. *Theoretical assumptions*

We consider downflow or upflow in a tube or annulus and proceed to determine the static instability point based on the minimum in the pressure drop vs flow rate characteristics (Fig. 1). We utilize essentially the standard flow equations of Meyer and Rose [8] and obtain a series of new analytical results.

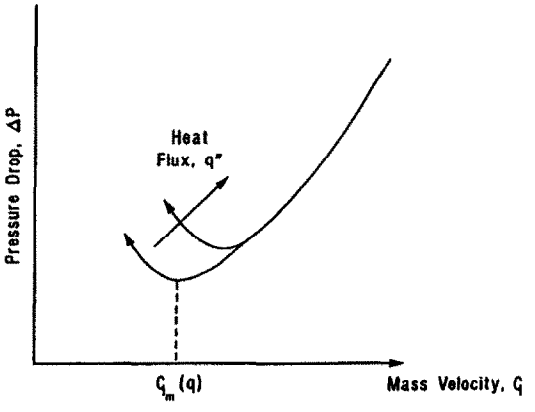

FIG. 1. Schematic of flow excursion (static instability) characteristic.

The following assumptions are made:

(1) The flow is one-dimensional with a uniform heat flux, q'', and is in a steady state.

(2) The relative velocity, if any, between the phases or components (i.e. bubbles and water) can be described by a slip or 'drift-flux' formulation.

(3) The irreversible wall friction and form pressure losses within the heated section can be characterized by an average (lumped) form loss and frictional multiplier, f.

(4) The downflow or upflow is caused by a constant pressure drop boundary condition, ΔP, imposed at the ends.

These assumptions enable the fundamental physics of the problem to be clarified and provide convenient and useful results.

2.2. *The general static instability criterion*

Consider now a flow of mass flux, G, and average density, ρ, in a tube or annulus with vertical upward ordinate, z. The *momentum* equation for the mixture of liquid plus vapor is

$$\frac{\partial G}{\partial t}+\frac{\partial}{\partial z}\left(\frac{G^2}{\rho}\right)=\frac{-\partial p}{\partial z}+\rho g\cos\theta-\frac{f\Phi^2}{2D_e}\left(\frac{G^2}{\rho}\right) \quad (1)$$

where Φ^2 is a two-phase multiplier and θ the angle between the vertical flow direction and gravity (0 deg for downflow and 180 deg for upflow).

For steady-state flow applicable to the static case, the first term is identically zero. Assuming an average value for f over the length z including entry losses, we may integrate equation (1) from inside the entrance at the origin $z = 0$, to the point of instability subject to the constant pressure drop boundary condition [4], to give

$$\Delta P=-\rho g z\cos\theta+\frac{f\Phi^2}{2D_e}\left(\frac{G^2}{\rho}\right)z+\left(\frac{1}{\rho_z}-\frac{1}{\rho_0}\right)G^2.$$

For the present analysis, the momentum flux given by the last term on the right-hand side is neglected, so that

$$\Delta P=-\rho g z\cos\theta+\frac{f_2}{D_e}\left(\frac{G^2}{2\rho}\right)z \quad (2)$$

where $f_2 = f\Phi^2$, an effective friction factor. The momentum flux is indeed usually small compared to the irrecoverable losses for the present considerations and can be included in the effective friction factor. Now, we take the static flow instability condition to be as observed in experiments, that is

$$\left.\frac{\partial(\Delta P)}{\partial G}\right|_z=0$$

$$\left.\frac{\partial^2(\Delta P)}{\partial G^2}\right|_z=\text{positive (a minimum)}.$$

Note that this definition does not rely on the external loop (supply) characteristics as usually written for the single-phase case, but is essentially analogous to the constant pressure drop Ledinegg conditions for upflow. For a pumped loop where the pressure drop is fixed by the external supply, and not, say, by having many parallel channels or a constant hydrostatic head, the condition is

$$\left.\frac{\partial(\Delta P)}{\partial G}\right|_z\leqslant\left.\frac{\partial(\Delta P)}{\partial G}\right|_{\text{supply}}.$$

Applying the instability condition to equation (2), we find the mass velocity, G_m, at the minimum to be given by a solution to the quadratic equation

$$\frac{f_2}{2D_e\rho^2}\left(\frac{\partial\rho}{\partial G}\right)G_m^2-\frac{f_2}{D_e\rho}G_m+g\cos\theta\left(\frac{\partial\rho}{\partial G}\right)=0$$

where the dependency of f_2 on G has been neglected. For the case where the pressure drop is set by the external supply, the right-hand side of this equation becomes $\partial(\Delta P)/\partial G|_{\text{supply}}$.

There are two roots for the solution for G_m from the above quadratic. These are

$$G_m=\frac{1}{\frac{1}{\rho}\left(\frac{\partial\rho}{\partial G}\right)}\left\{1\pm\left[1-\frac{2D_e}{f_2}\left(\frac{\partial\rho}{\partial G}\right)^2 g\cos\theta\right]^{1/2}\right\}. \quad (3)$$

If $D_e(\partial\rho/\partial G)^2 g\cos\theta/f_2\leqslant 1$, using the binomial expansion we find the non-trivial real solution to be the general stability criterion

$$G_m=\frac{g\rho D_e}{f_2}\cos\theta\left(\frac{\partial\rho}{\partial G}\right). \quad (4)$$

The two solutions are nearly equal in magnitude because the term corresponding to pure density instability, $2\rho(\partial G/\partial\rho)$, has been dropped consistent with the constraint $D_e(\partial\rho/\partial G)^2 g\cos\theta/f_2\leqslant 1$, which implies a bound on the heat flux. Evaluation of the constraint requires $(\partial\rho/\partial G)$ which we develop in Section 2.3 below. The available data used for comparison satisfy this constraint: zero gravity data should show the pure density instability only.

Let us examine the physical insights offered by this intuitively obvious result.

First, in *any* flow where $\partial\rho/\partial G$ is finite, the flow is inherently unstable and will exhibit a minimum value. Second, the minimum occurs where locally the irreversible pressure loss changes are comparable to, and offset by, incremental increases in the buoyancy forces, that is, $|fG\Delta G|\sim|g\rho\Delta\rho|$. Finally, this result is applicable to any fluid flow (single- or two-phase, two or three component, etc.) where the density changes with flow rate. We now proceed to examine specific formulations for the density variation for heated and unheated flows in a tube or annulus.

2.3. *Evaluation of the stability limit: diabatic two-phase flow*

In a two-phase flow of liquid and vapor (or gas), with cross-sectional average void fraction, α, the density is

$$\rho = (1-\alpha)\rho_l + \alpha\rho_g \tag{5}$$

or, as indicated by Zuber and Staub [6]

$$\partial\rho = -\Delta\rho_{lg}\partial\alpha \tag{6}$$

where

$$\Delta\rho_{lg} = \rho_l - \rho_g.$$

Thus

$$\frac{\partial\rho}{\partial G} = -\Delta\rho_{lg}\frac{\partial\alpha}{\partial G} \tag{7}$$

and the stability condition of equation (4) becomes

$$G_m = \frac{-D_e g\cos\theta\,\rho\Delta\rho_{lg}}{f_2}\left(\frac{\partial\alpha}{\partial G}\right). \tag{8}$$

Now, the *energy* equation is

$$\rho\frac{\partial h}{\partial t} + G\frac{\partial h}{\partial z} = q''\frac{A_w}{A_f}. \tag{9}$$

For steady-state flow, integrating with respect to z, the enthalpy rise is simply due to the wall heat flux

$$GA_f(h_z - h_{in}) = q''A_w. \tag{10}$$

Now

$$h_z = (1-X)h_f + Xh_g$$

where X is the vapor flow fraction, G_g/G. Rearranging equation (10)

$$GA_f(Xh_{fg} + \Delta h_{in}) = q''A_w \tag{11}$$

where $\Delta h_{in} = h_f - h_{in}$, and hence we have

$$X = \frac{-\Delta h_{in}}{h_{fg}} + \frac{q''A_w}{GA_f h_{fg}} \tag{12a}$$

which, for later convenience, we write as

$$X = X_{in} + X_e. \tag{12b}$$

Now, in a two-phase flow with relative velocity or slip ratio

$$S = \frac{u_g}{u_l}$$

$$\frac{1-X}{X} = \frac{1-\alpha}{\alpha}\frac{\rho_l}{\rho_g}\frac{1}{S} = \frac{1-\alpha}{\alpha}S^* \tag{13}$$

which enables us to derive an expression for $\partial\alpha/\partial G$ in terms of S and X, as

$$\frac{\partial\alpha}{\partial G} = \left(\frac{1}{X^*}\frac{\partial S^*}{\partial G} - \frac{S^*}{X^{*2}}\frac{\partial X^*}{\partial G}\right)\Big/\left(1+\frac{S^*}{X^*}\right)^2 \tag{14}$$

where

$$S^* = \frac{\rho_l}{\rho_g}\frac{1}{S}$$

and

$$X^* = \frac{1-(X_{in}+X_e)}{X_{in}+X_e}$$

which is a *general relation* for any heated two-phase flow with slip.

Evaluating the differentials, we have that

$$\frac{\partial X^*}{\partial G} = -\frac{1}{(X_{in}+X_e)^2}\frac{\partial X_e}{\partial G}$$

$$\frac{\partial S^*}{\partial G} = \frac{\rho_l}{\rho_g}\frac{\partial}{\partial G}\left(\frac{1}{S}\right)$$

and

$$\frac{\partial X_e}{\partial G} = -\frac{q''A_w}{A_f h_{fg} G^2}$$

so that equation (14) gives

$$\frac{\partial\alpha}{\partial G} = \frac{1}{\left(1+\dfrac{S^*}{X^*}\right)^2}\left[\frac{\rho_l}{X^*\rho_g}\frac{\partial}{\partial G}\left(\frac{1}{S}\right) - \frac{\rho_l q''A_w}{\rho_g S[1-(X_{in}+X_e)]^2 A_f h_{fg} G^2}\right]. \tag{15}$$

Therefore, the stability limit is, from equations (8) and (15)

$$G_m = -\frac{\rho\rho_l D_e\cos\theta\, g\Delta\rho_{lg}}{\rho_g f_2\left(1+\dfrac{S^*}{X^*}\right)^2}\left[\frac{1}{X^*}\frac{\partial}{\partial G}\left(\frac{1}{S}\right) - \frac{q''A_w}{S[1-(X_{in}+X_e)]^2 A_f h_{fg} G_m^2}\right] \tag{16a}$$

subject to the constraint given in Section 2.2 above, which we can now evaluate as

$$\left[\frac{\Delta\rho_{lg}\rho_g A_w q''}{(X_{in}+X_e)^2\rho_l h_{fg} G^2 A_f}\right]^2\frac{D_e g\cos\theta}{f_2} \leqslant 1 \tag{16b}$$

which at high qualities, $X_e \gg X_{in}$, becomes

$$q'' \geqslant \frac{\rho_g h_{fg} D_e^{3/2}(g\cos\theta)^{1/2}}{2\sqrt{2} f_2^{1/2} L} \tag{16c}$$

and at low qualities, $X_{in} \gg X_e$, is

$$q \leqslant \frac{D_e^{1/2} G^2 \Delta h_{in}^2 f_2^{1/2}}{4\Delta\rho_{lg}\rho_g SL(g\cos\theta)^{1/2}}. \tag{16d}$$

This is an interesting and *general* implicit result, showing how G_m varies with friction, water temperature, pressure, and slip.

2.4. *Limiting solutions*

The first term in brackets involving the slip derivative is difficult to evaluate exactly, but is expected to

be of small magnitude. We proceed to evaluate the limits of equation (16): the simplest case we take is the limit when

$$\frac{\partial S^*}{\partial G} \Rightarrow 0.$$

Hence, from equation (16a) the minimum mass flux is

$$G_m = \frac{\rho D_e g \cos\theta \rho_l \Delta\rho_{lg} q'' A_w}{f_2 (X_{in}+X_e)^2 S \rho_g A_f h_{fg} G_m^2 (X^*+S^*)^2} \quad (17)$$

and we note that a useful approximation is $X^* \simeq (X_{in}+X_e)^{-1}$.

We can write equation (17) in terms of the ratio of the *local* gravitational ($g\Delta\rho_{lg}\cos\theta$), and frictional $-(f_2 G^2/2D_e\rho)$, pressure gradients ΔP^* as

$$G_m = \Delta P^* \frac{2\rho_g S q'' z}{\rho_l h_{fg} D_e (X_{in}+X_o)^2} \quad (18)$$

a key result for both upflow and downflow. In order to evaluate the slip ratio, we may take one of the conventional formulations, i.e.

$$S = f(\rho_l/\rho_g) \simeq (\rho_l/\rho_g)^n \quad (19)$$

where $1/2 \leqslant n \leqslant 1/3$. In the low quality limit, $X_e \ll X_{in}$, and we can rewrite equation (18) in the convenient non-dimensional form

$$N_s = \left[\frac{S\Delta P^*}{2}\right] \frac{z}{L_l} \frac{\Delta\rho_{lg}}{\rho_l} \quad (20)$$

where L_l is the non-boiling liquid length, $D_e G_m \Delta h_{in}/4q''$. Now, since $\Delta\rho_{lg} \simeq \rho_l$

$$N_s = \left[\frac{S\Delta P^*}{2}\right] L^* = CL^*, \quad (21)$$

say, where

$$N_s = \frac{\Delta\rho_{lg}\Delta h_{in}}{N_s \rho_g h_{fg}}, \quad (22)$$

a subcooling number

$$\Delta P^* = \left(\frac{\partial P}{\partial z}\right)_g \Big/ \left(\frac{\partial P}{\partial z}\right)_f,$$

the critical pressure gradient number at instability, and

$$L^* = \frac{z}{L_l},$$

the instability to non-boiling length number.

Similarly, our general result for subcooled boiling (equation (17)) can be written, using equation (19)

$$\Delta P^* = \frac{X^2}{X_e}\left(\frac{\rho_g}{\rho_l}\right)^{n-1}. \quad (23)$$

Equations (18), (21), and (23) show the parameter dependencies, and they show that the *local* gradients dominate the flow instability. These new results (equations (16)–(23)) are quite novel and testable, and in particular predict a linear dependency on power density and a non-linear effect of inlet subcooling.

We note that the parameter L^* is equivalent to Whittle and Forgan's [2] correlating parameter, R, which they found to be constant for their data range. We have shown, therefore, a theoretical basis for their entirely empirical observational result.

The instability length number, L^*, represents the length of boiling that exists before instability occurs; indeed, Durant and Ward [19] noted that some 0.5 m could be in nucleate boiling in a several-meter-long channel. Obviously, for highly subcooled flows, subcooled nucleate boiling can occur as also observed by Whittle and Forgan [2] and Costa *et al.* [10].

One further limit is of interest, which is when the inlet flow is near saturation. Since, $X_{in} \to 0$, $X^* \to (1-X_e)/X_e$ and recalling that $S^*/X^* \gg 1$, therefore, equation (16) becomes, in the saturated limit

$$G_m = \frac{D_e^2 g \Delta\rho_{lg}\rho_g h_{fg}}{f_2 S^2 q'' z} \quad (24)$$

which predicts an inverse length dependency which we examine in Section 3.

3. COMPARISONS WITH DATA

3.1. *Available world data base*

To test the theory we proceed to systematically evaluate the predicted dependencies. Data are rather scattered in the literature, particularly for downflow, but we proceed to analyze carefully the available information to check the theory, its results and assumptions. Not all the data have the required constant pressure drop conditions between the inlet and outlet because of inlet flow throttling or orificing, or a bypass flow. We selected data for water flow that were consistent with this restraint or had an unthrottled inlet flow. The salient features of the experiments are summarized in Table 1. The flow rates were converted to mass fluxes in order to be consistent with the theoretical basis.

For the data of Costa *et al.* [10], Mirshak [20], and Qureshi *et al.* [17], the values of G_m were straightforwardly read directly from the graphs given; the test section dimensions were taken as quoted. However, Whittle and Forgan [2] actually tabulated their one series of downflow data (and the upflow data) as a derived temperature rise ratio. The actual flow rates were, therefore, back calculated, assuming that the quoted powers simply go to water heating in accord with the temperature ratios given in their table of results. We also utilize the upflow data with a range of D_e and test section lengths, where the equivalent diameters are based on the heated perimeter.

The report of Durant and Ward [19] does not quote a test section diameter or dimension other than length, and, therefore, these data were not pursued further. The results tabulated by Chen and King [21] are par-

Table 1. Available world data

Authors	Type—Flow direction	Test section D_e (-10^{-3} m)	Test section L (m)	Test range Pressure (MPa)	Test range Heat flux (kW m^{-2})	Test range Mass flux (kg m^{-2} s^{-1})
Costa *et al.* (1967) [10]	Channel—up	38	0.6	0.17	200–4000	150–6900
Mirshak (1958) [20]	Tube—down	6.2	4.267	0.10	195–1248	879–4883
		9.44	4.267	0.10	446–1715	1221–4883
Whittle and Forgan (1967) [2]	Channels up and down tube—up	2.79–6.45	0.41	0.12	420–1480	917–9840
			0.61	0.17		
Qureshi *et al.* (1989) [17]	Annulus/tube—down	31.75	1.83	0.14	69–274	2593–11 161
		18.8	2.44	0.24	1262–3156	146–533
				0.45		1792–4992
Chen and King (1989) [21]	Annulus/tube—down	6.8	3.57	0.19	1540–2830	4258–9712
		12.7				
D'Arcy (1967) [22]	Parallel/tube—up	13.26	3.05	7.0	275–893	293–1318
Masini *et al.* (1968) [23]	Parallel/annulus—up	20–30	3.00	1.0	30–400	180–370
				3.0		
				5.0		
Nylund *et al.* (1969, 1970) [24, 25]	Tube bundle—up	36.6	4.37	5.2	480–900	570–820
Enomoto *et al.* (1985) [26]	Parallel/bundle—up	20.5	3.71	6.86	366–811	278–660

ticularly interesting, being for a heated tube centered within a tube to form an annulus. The values for G_m are both tabulated and can be read from the original graphs for simultaneous instabilities in both the tube and the annulus. The test section dimensions are directly quoted.

For the data of D'Arcy [22], the results were read directly from the 'carpet plots' given in the original paper and for Masini *et al.* [23] from the tabulated values. The data of Nylund *et al.* [24, 25] are for a large tube bundle in a natural circulation loop (the FRIGG tests), and the data were taken from the tables given for the instability results.

The data of Enomoto *et al.* [26] are for the case of vertical upflow through parallel rod bundles. The main bundle had four heated rods and the bypass bundle had nine heated rods. The data were read from plots given in Enomoto *et al.*'s paper. All geometric data are also given in the text.

The data of Toyoda [27], Dormer and Bergles [28], and Maulbetsch and Griffith [29] are available but are for horizontal channels where the pressure drop was set by the external (pump) supply. The pressure drop vs flow characteristics for the supply are, in general, not available. Our theoretical development and interests lie in the parallel channel and natural circulation case. Therefore, these horizontal data are outside our areas of interest.

For all the above tests, it is not always clear in the original references that an *exactly* constant pressure drop boundary condition was maintained via, for example, a large bypass flow or constant hydrostatic head. Thus, the individual experimental loop, valve and pump characteristics may have impacted the results, particularly beyond instability. This is often manifested by the upward turn in the pressure drop characteristics; whereas, ideally, this should turn horizontally at a constant ΔP. The onset of instability is taken as variously reported and defined in the experiments: from the pressure drop and flow characteristics, from the unstable flow and periodic fluctuations before burnout, and from extrapolation of the 'noise' spectrum signature to the point of instability.

All these data satisfy the constraint given by equation (16), to within 5%, thus justifying the approximation in the derivation of the stability criterion.

3.2. *Comparison of theory with power density, hydraulic diameter, and length effects*

For the above experiments, which have been performed for water flow with uniform heat fluxes, the theory (equation (18)) suggests we should plot the mass flux at the minimum, G_m, vs the power density, q''/D_e, which we show in Figs. 2(a) and (b). We see that, immediately, the theory predicts a straight line and agrees with a given data set. The dependency on inlet subcooling is shown in Figs. 3(a) and (c). A slight nonlinearity, as predicted by equation (18) is evident.

We also predict a systematic variation with inlet subcooling, which we illustrate in Fig. 3, for a wide range of pressure when we plot according to the theoretical suggestion $G_m D_e/q''$.

The linear variation with D_e is also supported by the data of Costa *et al.* [10] for a given subcooling.

Collapsing the data further, we take for comparison purposes $z \equiv L$ in equation (24) to remove the effect of test section length. In Fig. 4, we show how q''/D_e is in *exact* agreement with the predicted variation as

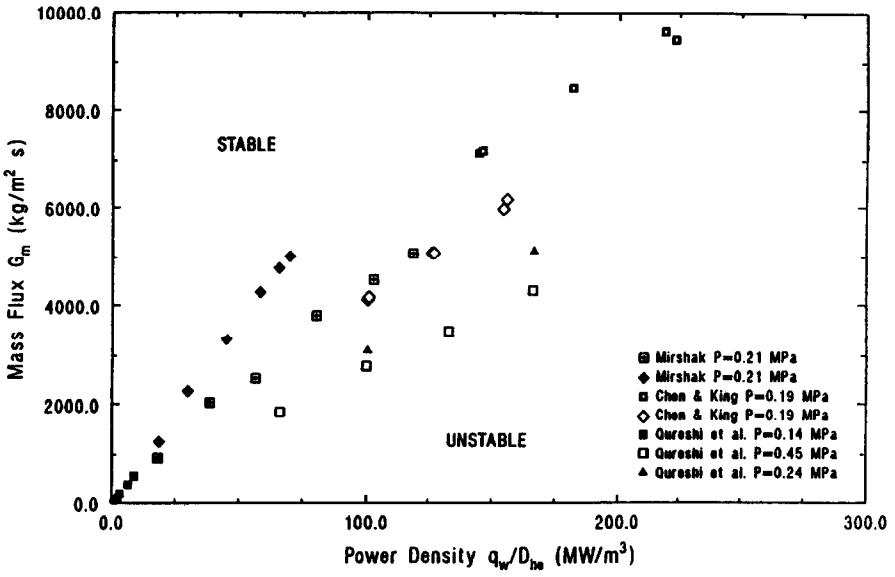

FIG. 2(a). Minimum mass flux as a function of power density at constant operating conditions.

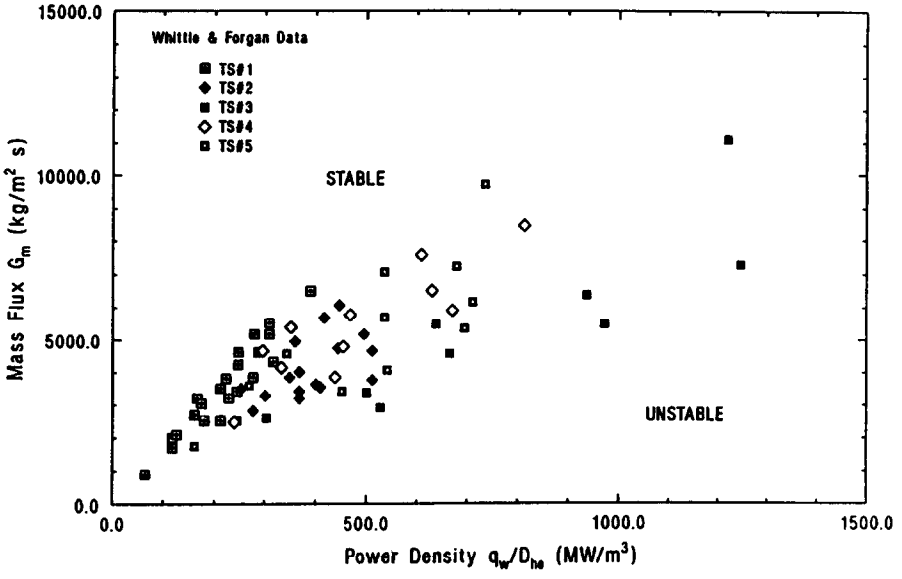

FIG. 2(b). Minimum mass flux as a function of power density at various operating conditions.

$1/L$, with $G_m \to 0$ as $L \to \infty$, for the complete constant head data set of Mathison [30], where the theory is simply fitted to just one point (at 2.30 m) since G_m was not given.

For a given test-section geometry (L and D_e fixed), and for a given operating pressure and inlet subcooling, equation (18) predicts that the ratio $G_m/(Lq''/D_e)$ or (G_m/q'') is a constant for the case $X_e < X_{in}$. The available experimental data show exactly this property. This observation is illustrated in Table 2 for several of the experimental investigations from the literature. The implication is that ΔP^* is a fundamental property of instability in a given test section. With this information, experiments need only be conducted to determine this ratio at one operating point. Then, the minimum flow, G_m, at any other heat flux is calculated from the experimentally determined ratio. Reduction of the available experimental data for use in the present report indicates that, usually, several tests are run at fixed pressure and inlet condition over a range of mass flux and heat flux. This procedure is no longer necessary. Instead, tests need to cover a range of inlet subcooling values. Then, the values of G_m for other values of q'' at the tested values of inlet subcooling are determined from the value of the ratio.

3.3. *Comparison of theory with pressure effects*

In this section we investigate the effect of pressure on the stability. The data used in this work include

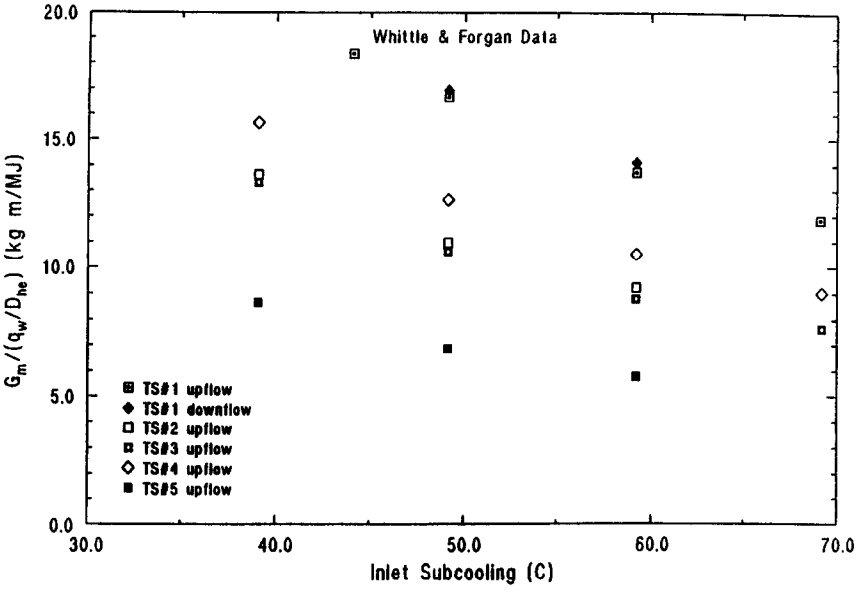

FIG. 3(a). Theoretical parameter, $G_m/(q_w/D_{he})$, as a function of inlet subcooling.

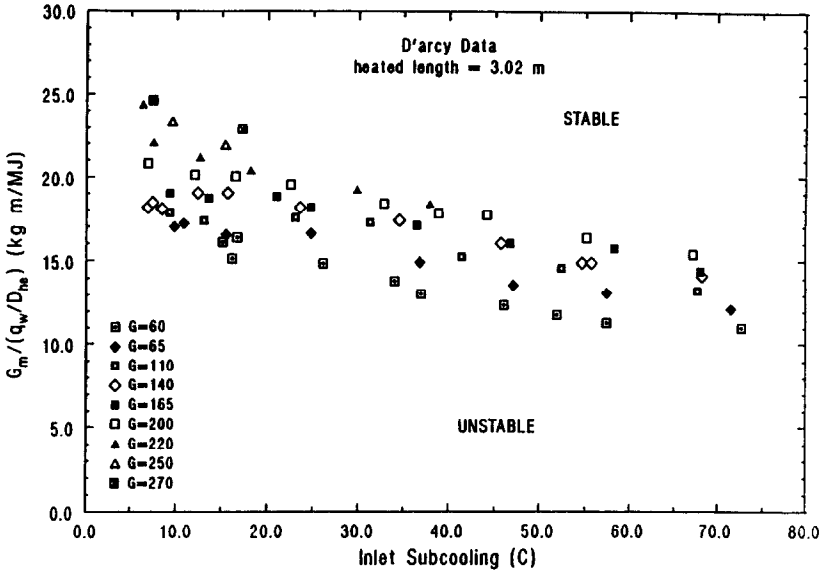

FIG. 3(b). Theoretical parameter, $G_m/(q_w/D_{he})$, as a function of inlet subcooling.

low (0.10–0.50 MPa) and high pressure (1.0–7.0 MPa). However, these data also fall into two categories relative to the equilibrium quality at instability. That is, the low pressure data correspond to very low quality (below saturation in most cases) and the high pressure data correspond to net vapor generation conditions ($0.10 \leqslant X \leqslant 0.80$).

The assumptions used in the development of the theoretical model resulted in approximating the distinctive effect of two-phase friction slip and momentum flux. These effects are known to be functions of the void fraction, mass flux, and pressure level (through the density ratio, transport properties, etc.). Although these effects can be incorporated, present knowledge introduces a certain empiricism into the model that would be difficult to sort out at the data-comparison level. We expect, though, that these two-phase flow effects will be different for the low quality and the high quality regimes, corresponding to the slip and friction for subcooled and saturated forced convective boiling, respectively.

The theoretical model suggests, by use of equation (23), that

$$\Delta P^* = \frac{(X_{in}+X_e)^2}{X_e}\left(\frac{\rho_l}{\rho_g}\right)^m \tag{25}$$

subject to the constraint of equation (16).

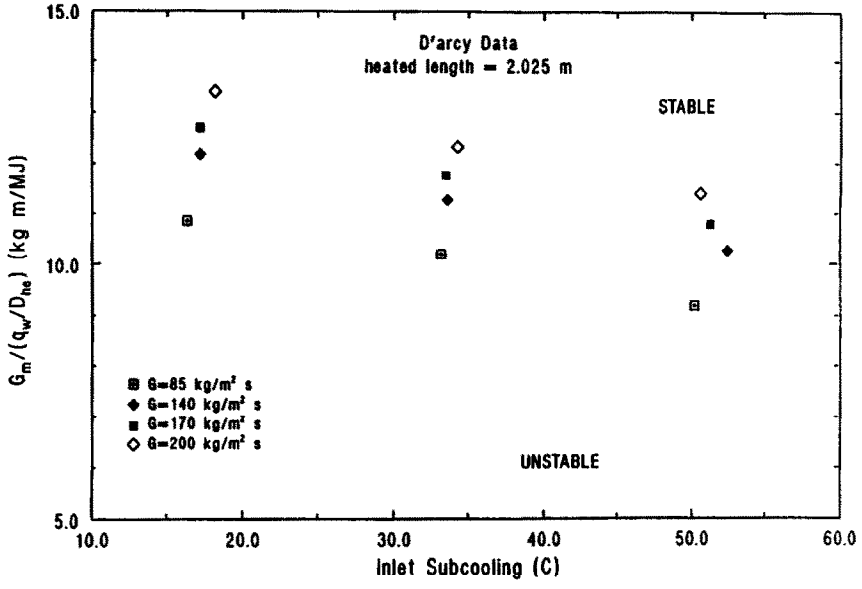

FIG. 3(c). Theoretical parameter, $G_m/(q_w/D_{he})$, as a function of inlet subcooling.

The effect of pressure is shown in Fig. 5. The data of Nylund *et al.* [24, 25], Enomoto *et al.* [26], Masini *et al.* [23], and D'Arcy [22] are shown as a function of the equilibrium exit quality with ΔP^* calculated from equation (25). The data collapse to a compact cluster if the density ratio (ρ_l/ρ_g) is used to the one-third power. This represents only a preliminary estimate of the two-phase friction multiplier, slip, and momentum flux effects. The data do form a much more compact grouping, however, and a more detailed accounting of the two-phase multiplier is suggested.

The low pressure, low quality data are shown in Fig. 6 in the form of equation (25). Most of the data points are from Whittle and Forgan [2]; a few data from other test sections are also shown. The density ratio correction pulls the non-Whittle and Forgan data into alignment but not into agreement with the Whittle and Forgan data. A straight line through the data is shown in Fig. 6.

The results given in Figs. 5 and 6 suggest that $\Delta P^*(\rho_l/\rho_g)^m$ forms one basis for correlating the experimental data. The straight line in Fig. 5 is given by $2.5(X_{in}+X_e)$; and that in Fig. 6 is $-4.0(X_{in}+X_e)$. Putting these results into equation (25), the minimum mass flux is given by the implicit result

$$G_m = \frac{bq''A_w}{(X_{in}+X_e)A_f h_{fg}}\left(\frac{\rho_g}{\rho_l}\right)^{1/3} \qquad (26)$$

with $b = 2.5$ for $(X_{in}+X_e) > 0$ and $b = -4.0$ for $(X_{in}+X_e) < 0$.

These results are preliminary and only account for two-phase flow effects in an approximate manner. For general correlating or design purposes, an *iterative* approach should be utilized, in which successive approximations for G_m are used to evaluate the X_e term in equation (26). For specific test sections or design operation condition, it is recommended that the quantity $(G_m/q''D_e)$ be correlated vs inlet enthalpy or subcooling as illustrated in Fig. 3.

4. DISCUSSION

4.1. *Remarks on the theory*

We have shown the inherent static instability of two-phase flows and the importance of key parameters particularly of the heat flux, pressure drop ratio, and pressure. As can be seen from the theory, adiabatic two-phase flows are also unstable.

We conclude the result is not dependent on the occurrence of the first voids, as in subcooled boiling, and would not expect a priori the Saha and Zuber [18] correlation, or modifications of it, to apply as an 'indicator of stability'. The occurrence of instability may well be close to this point, but certainly does not coincide with it (i.e. $L^* < 1$ always).

The empirical correlation of Whittle and Forgan [2] for rectangular channels of width, W, and breadth, B (their equation (1)), can be recast in the form, for cgs units

$$\frac{2q''(W+B)L}{G_m c_p WB} = R, \quad \text{a constant} \sim 0.7. \qquad (27)$$

This constant, R, corresponds to the instability length, L^*, in equation (22) as we have previously noted. Rearranging, we find, for current SI units

$$G_m = 57\frac{q''L}{D_e h_l}. \qquad (28)$$

This indicates, by comparison of equation (28) to equation (18) with $z \equiv L$, a fundamental similarity but that the constant should in fact be physically

Table 2. Illustration that $G_m/(Lq_w/D_{he})$ is constant for given geometry and operating point

Test section reference	Geometry	Pressure (MPa)	Inlet temperature (K)	Heat flux range (kW m^{-2})	Mass flux range (kg m^{-2} s^{-1})	Range of G (Lq_w/D_e) (kg MJ^{-1})
Whittle and Forgan [2] upflow	Rectangular channel $L = 0.522$ m $D_e = 2.79 \times 10^{-3}$ m	0.12	328.15	930–1700	4208–7697	23.70–23.72
Whittle and Forgan [2] upflow and downflow	Rectangular channel $L = 0.610$ m $D_e = 6.45 \times 10^{-3}$ m	0.12	318.15	780–2040	917–4320	22.69–22.98
Qureshi *et al.* [17] downflow	Round tube $L = 2.44$ m $D_e = 18.92 \times 10^{-3}$ m	0.45	298.15	1262–3155	1782–4143	10.18–11.01
Qureshi *et al.* [17] downflow	Annulus $L = 1.829$ m $D_e = 31.75 \times 10^{-3}$ m	0.14	343.15	69.4–274.5	146–534	30.02–36.4
Chen and King [21] downflow	Round tube $L = 3.57$ m $D_e = 12.7 \times 10^{-3}$ m	0.19	305.15	1640–2470	6937–9712	12.30–13.30
Chen and King [21] downflow	Annulus $L = 3.57$ m $D_e = 15.12 \times 10^{-3}$ m	0.19	305.15	1540–2330	4058–5767	10.48–11.13
Nylund *et al.* [24] FRIGG-1 upflow	6-Rod bundle $L = 4.38$ m $D_e = 42.42 \times 10^{-3}$ m	5.0	531	965.5–1074	796–891	7.98–8.40
Nylund *et al.* [24] upflow	36-Rod bundle $L = 4.365$ m $D_e = 36.60 \times 10^{-3}$ m	5.0	531–534	850–907	700–725	6.52–6.95
Enomoto *et al.* [26] upflow	4-Rod bundle $L = 3.71$ m $D_e = 20.5 \times 10^{-3}$ m	6.86	535–536	384–811	278–660	3.98–4.87

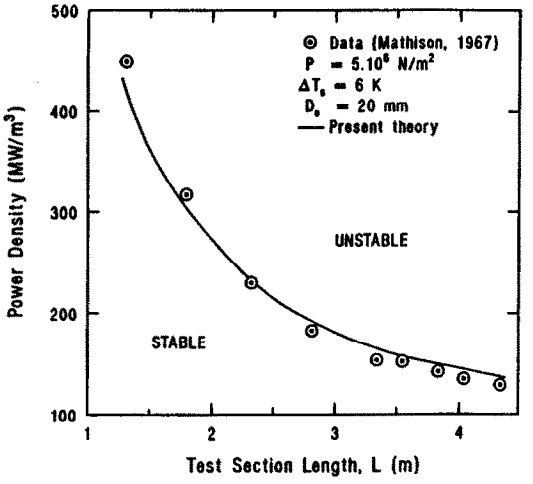

FIG. 4. Comparison of theory and experiment: variation of power density at hydrodynamic instability with test section length.

based. However, the physical interpretation is very different in the sense that the present theory considers the pressure drop due to voids and the effect of *evaporation* (h_{fg}); whereas, the Whittle and Forgan correlation implies only *heating* (h_l).

We also compare to the analysis of Ishii and Zuber [11] for *dynamic* instability. By perturbation analysis of the conservation laws for upflow, the result can be stated as an identity [9]

$$N_p - N_s = X_e \frac{\Delta\rho_{lg}}{\rho_g}. \tag{29}$$

There N_p and N_s are the phase-change and subcooling numbers, respectively, and X_e the equilibrium exit quality. Recasting this result using the present nomenclature, for low qualities where $G \simeq \rho_l u_l$, we obtain

$$G_m = \frac{q'' z}{h_{fg} D_e (X_e + h_l/h_{fg})} \tag{30}$$

which is just the identity for X_e we have utilized for *static* instability (equation (12)). Saha *et al.* [9] showed that the onset of *dynamic* instability (oscillations) was bounded by equation (29) for high subcoolings ($N_s \geqslant 2$), which certainly covers our data range and water temperatures.

At low subcoolings ($N_s \leqslant 2$), Saha *et al.* [9] adopted a lower limit as given by the Saha and Zuber [18] subcooled boiling correlation

$$N_s = 1.54 \left(\frac{D_e}{z}\right) N_p \tag{31}$$

which may be conveniently simplified and rewritten as, for current SI units

$$G_m = 154 \frac{q''}{h_l}. \tag{32}$$

This expression is also remarkably similar in form to that derived above for static instability as given by Whittle and Forgan [2] (see equation (28)), except for the dramatic difference in the magnitude of the constants (see also Ruggles [31]) for typical ranges of L/D_e.

Thus, these comparisons show the following:

(1) Dynamic and static instabilities are related in the form of the expressions for onset, especially for higher subcoolings ($N_s \geqslant 2$).

(2) Non-equilibrium subcooled boiling occurs, according to the Saha–Zuber correlation, at mass

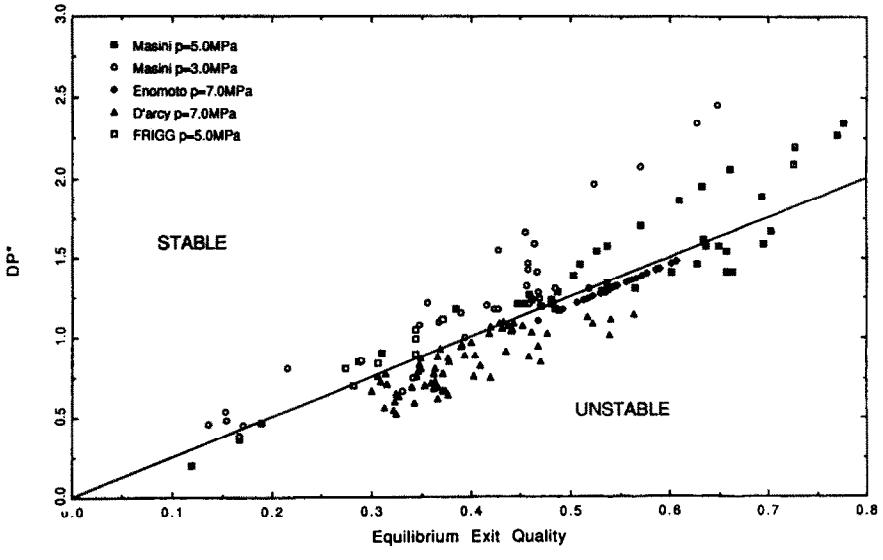

FIG. 5. Correlation of pressure effect.

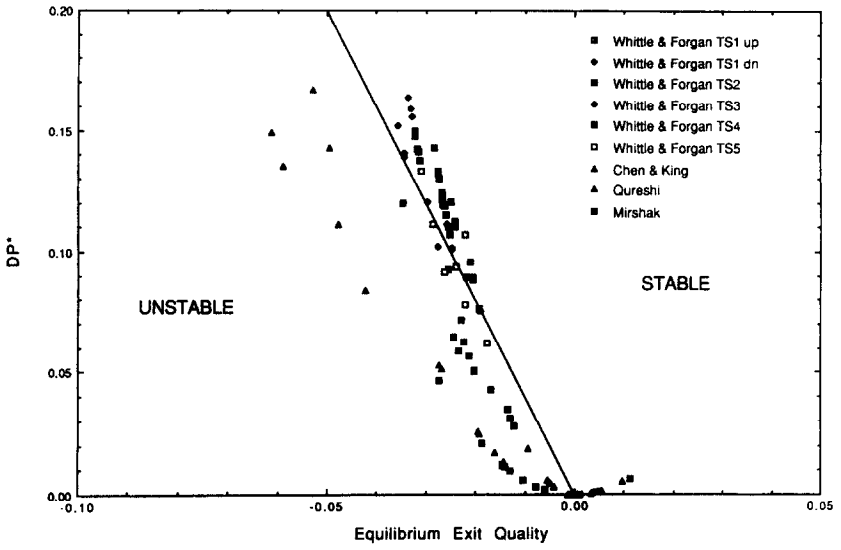

FIG. 6. Low pressure, low exit quality data correlation.

velocities very much higher than that at which static instability occurs.

(3) Downflows and upflows are entirely analogous for the theoretical treatment of static instability.

The new mass velocity correlation developed here should now be extended using data for a wider range of subcoolings and pressures, via the dependencies suggested by the more general result (equation (16a)).

4.2. *Non-equilibrium boiling effects*

The present analysis is based on thermal equilibrium estimates of quality, X_e, despite the obvious fact that the *actual* voids are reduced by vapor condensation.

In order to illustrate the effect of nonequilibrium, we take for simplicity the Levy [32] approach to the 'true' or reduced non-equilibrium quality, X_{Ne}, namely

$$X_{Ne} = X - \left(\frac{h_{lz}}{h_{fg}}\right)\exp\left(\frac{X}{X_d} - 1\right) \qquad (33)$$

where X_d is the (negative) quality at bubble 'departure'. Utilizing this correction, the relevant differential in equation (14) becomes

$$\frac{\partial X_{Ne}}{\partial G} = \frac{\partial X}{\partial G}\left[1 - \exp\left(\frac{X}{X_d} - 1\right)\right] + \left[\frac{X}{X_d} - 1\right]\frac{\partial X_d}{\partial G}\exp\left(\frac{X}{X_d} - 1\right) \qquad (34)$$

showing a small reduction from equilibrium of order of 10–20%, at most.

For the simplest cases when $\partial X_d/\partial G \to 0$

$$\frac{\partial X_{Ne}}{\partial G} \simeq \frac{\partial X}{\partial G}\left[1 - \exp\left(\frac{X}{X_d} - 1\right)\right] \qquad (35)$$

and we should strictly correct G_m in equation (18) by the term in brackets on the right-hand side of equation (35), leading to a slight increase. However, our comparisons with data already implicitly include this correction in the constant.

4.3. *Recovery from instability*

It is also possible to speculate on whether the surface and flow could return to a stable condition having once become unstable. In a transient, we have shown that the conditions for instability should depend on the inlet flow parameters ρ_g, Δh_{in}, and the instantaneous thermodynamic properties (h_{fg}, ρ_g), etc. A steady-state correlation, such as equations (28) and (32), will not show these dependencies.

Provided the wall has not overheated to the point where rewetting is very slow, the theory permits recovery if conditions cause the flow rate to exceed G_m. The recovery path may show hysteresis, depending on whether it is the pressure drop or flow rate which is increasing again. Experiments to confirm the existence of the hysteresis are desirable.

5. CONCLUSIONS

We have shown that flow in a heated annulus, tube, or rod bundle channel is unstable. The necessary and sufficient condition has been derived analytically in the form of a general result. The predictions of the theory are in agreement with the available data, and a new theoretically-based correlation for the mass velocity at static instability has been obtained. The

experimental data cover the ranges $D_e = 6$–35 mm, $q_w = 30$–3200 kW m^{-2}, $G_m = 150$–$11\,000$ kg m^{-2} s^{-1}, $L = 0.40$–4.40 m, and pressure from 0.10 to 7.0 MPa.

The theoretical basis of the correlation has been shown to be in agreement with experimental data. The mass flux to power density ratio is linear, and the theoretical results correctly predict the dependence on length, inlet subcooling, and pressure.

Predictions of the theory show the physics to be determined by the ratio of the gradients of the buoyancy to irrecoverable frictional forces. This demonstrates that the increased local pressure drop due to the boiling flow is the key effect that causes the instability.

Design variations are possible for delaying the onset, such as increasing length, pressure, and hydraulic diameter. The theory indicates that the instability is not uniquely determined by, or related to initiation of subcooled boiling, and that two-phase flows are always unstable at some point.

Acknowledgments—This work was supported under DOE Contract No. DE-AC07-76IDO1570. The authors are grateful to the reviewers for comments regarding clarification of the constraint on the new analytical solution presented here as the stability criterion.

REFERENCES

1. R. B. Duffey and E. D. Hughes, Dryout stability and inception at low flowrates, *Int. J. Heat Mass Transfer* (1991).
2. R. H. Whittle and R. Forgan, A correlation for the minima in the pressure drop versus flow-rate curves for sub-cooled water flowing in narrow heated channels, *Nucl. Engng Des.* **6,** 89–99 (1967).
3. W. R. Gambill and R. D. Bundy, Heat transfer studies of water flow in thin rectangular channels, Parts I and II, *Nucl. Sci. Engng* **18,** 69–89 (1964).
4. E. R. Quandt, Analysis and measurement of flow oscillations, *Chem. Engng Prog. Symp. Ser. 57* **32,** 111–126 (1961).
5. N. Zuber, Flow excursions and oscillations in boiling, two-phase flow systems with heat addition, *Proc. Symp. on Two-phase Flow Dynamics*, EUR 4288e, Vol. II, pp. 1071–1109 (1967).
6. N. Zuber and F. W. Staub, An analytical investigation of the transient response of the volumetric concentration in a boiling forced-flow system, *Nucl. Sci. Engng* **30,** 268–278 (1966).
7. E. P. White and R. B. Duffey, A study of the unsteady flow and heat transfer in the reflooding of water reactor cores, *Ann. Nucl. Energy* **3,** 197–210 (1976).
8. J. E. Meyer and R. P. Rose, Application of a momentum integral model to the study of parallel channel boiling flow oscillations, *Trans. ASME, J. Heat Transfer* **85,** 1–9 (1963).
9. P. Saha, M. Ishii and N. Zuber, An experimental investigation of the thermally induced flow oscillations in two-phase systems, *Trans. ASME, J. Heat Transfer* 616–622 (1976).
10. J. Costa, M. Courtaud, S. Elberg and J. Lafay, La redistribution de débit dans les réacteurs de recherche, *Bull. Inform. Sci. Tech.* Commisariat à l'Energie Atomique, No. 117, 89–103 (1967).
11. M. Ishii and N. Zuber, *Proc. Fourth Int. Heat Transfer Conf.*, Vol. 5, B.511 (1970).
12. R. T. Lahey and A. Yadigaroglu, NUFREQ, a computer program to investigate thermo-hydraulic stability, General Electric Co., NEDO-13344 (1973).
13. L. Moberg and K. Tangeir, Time domain BWR stability analysis using the 3-D code RAMONA-3B, *Trans. European Nucl. Conf.*, Vol. 3 (1986).
14. F. Araya, K. Yoshida, M. Hirano, K. Matsumoto, M. Yokobayashi and A. Kohsaka, RETRAN calculations on the BWR instability, Stability Symp., Idaho National Engineering Laboratory, EG&G Idaho, Inc. (1989).
15. R. R. Galer and P. J. Jensen, The sensitivity of BWR stability analyses to nodal boiling boundary location, Stability Symp., Idaho National Engineering Laboratory, EG&G Idaho, Inc. (1989).
16. J. G. M. Anderson, J. C. Shaug and A. L. Wirth, TRACG time domain analysis of thermal hydraulic stability sensitivity to numerical method and comparison to data, Stability Symp., Idaho National Engineering Laboratory, EG&G Idaho, Inc. (1989).
17. Z. H. Qureshi, B. S. Johnston and K. Chen, Flow instability in vertical heated tubes under downflow conditions, *Proc. ANS Workshop on Safety of Uranium–Aluminum Fueled Reactors*, Idaho Falls, Idaho, 14–16 March (1989).
18. P. Saha and N. Zuber, Point of net vapor generation and vapor void fraction in subcooled boiling, *Proc. Fifth Int. Heat Transfer Conf.*, Vol. 4, pp. 175–179 (1974).
19. W. S. Durant and D. A. Ward, Critical effluent temperature for initiation of flow instability, DOE Report DPST-63-153 (1963).
20. S. Mirshak, Transient flow of boiling water in heated tubes, DOE Report DP-301TL (1958).
21. K. F. Chen and J. F. King, Flow TRAN benchmarking with onset of flow instability data from 1963 Columbia University experiments, DOE Report DPST-88-666 (1989).
22. D. F. D'Arcy, An experimental investigation of boiling channel flow instability, *Proc. Symp. on Two-phase Flow Dynamics*, EUR 4288e, Vol. II, pp. 1173–1223 (1967).
23. G. Masini, G. Possa and F. A. Tacconi, Flow instability thresholds in parallel heated channels, *Energ. Nucl.* **15,** 777–786 (1968).
24. O. Nylund, K. M. Becker, R. Eklund, O. Gelius, A. Jensen, D. Malnes, A. Olsen, Z. Rouhani and F. Akerhielm, Hydrodynamic and heat transfer measurements on a full-scale simulated 36-rod Marviken fuel element with non-uniform axial and radial heat flux distribution, AB-Atomenergi ASES-Atom Report FRIGG-4, R4-502/R1-1253 (1970).
25. O. Nylund, K. M. Becker, R. Eklund, O. Gelius, I. Haga, A. Jensen, D. Malnes, A. Olsen, Z. Rouhani, J. Skaug and F. Akerhielm, Hydrodynamic and heat transfer measurements on a full-scale simulated 36-rod Marviken fuel element with non-uniform radial heat flux distribution, AB-Atomenergi ASEA-Atom Report FRIGG-3, R4-494/R1-1154 (1969).
26. T. Enomoto, S. Muto, T. Ishizuka, A. Tanabe, T. Mitsutake and M. Sakurai, Thermal hydraulic stability experiments in rod bundle, *Proc. Third Int. Topical Meeting on Reactor Thermal Hydraulics*, 9.B, Newport, Rhode Island (1985).
27. K. G. Toyoda, HW-28527, Pressure drop characteristics of two-phase non-isothermal flow in small diameter tubes, Hanford Atomic Products Operation, HW-28527 (1953).
28. T. Dormer, Jr. and E. A. Bergles, Pressure drop with surface boiling in small-diameter tubes, Technical Report No. 8767-31, Department of Mechanical Engineering, Massachusetts Institute of Technology (1964).
29. J. S. Maulbetsch and P. Griffith, A study of system-induced instabilities in forced-convection flows with subcooled boiling, Technical Report No. 5382-35, Depart-

ment of Mechanical Engineering, Massachusetts Institute of Technology (1965).
30. R. P. Mathison, Out of pile channel instability in the loop Skalvan, *Proc. Symp. on Two-phase Flow Dynamics*, EUR 4288e, Vol. II, pp. 1999–2064 (1967).
31. A. Ruggles, Flow excursion considerations in ANS and HFIR, *Proc. ANS Workshop on Safety of Uranium–Aluminum Fueled Reactors*, Idaho Falls, Idaho, 14–16 March (1989).
32. S. Levy, Forced convection subcooled boiling prediction of vapor volumetric fraction, *Int. J. Heat Mass Transfer* **10**, 951–965 (1967).

APPARITION DE L'INSTABILITE D'UN ECOULEMENT PERMANENT DANS LES TUBES, CANAUX, ESPACES ANNULAIRES ET LES GRAPPES DE CYLINDRES

Résumé—Un modèle théorique est développé pour l'apparition de l'instabilité d'écoulement vertical montant ou descendant d'un fluide en ébullition dans un canal, à perte de pression constante. Le modèle est basé sur les équations de bilan de quantité de mouvement et d'énergie avec une modélisation algébrique des effets diphasiques de glissement de vitesse. Les prédictions de la théorie sont testées par des données expérimentales pour les effets de la pression, du flux thermique, de la longueur, du sous-refroidissement d'entrée et de la qualité du fluide à la sortie. Les prédictions de la dépendance du flux de masse minimal sur ces variables sont en accord complet avec les expériences. Celles-ci concernent les géométries de tube cylindrique, de canal rectangulaire, d'espace annulaire et de grappe de cylindres, avec montée ou descente verticale, sous des conditions de non ébullition du coeur et de génération nette de vapeur. La collection de données fournie ici apparait être la plus complète de ce qui est connu. Les résultats théoriques suggèrent une méthode pour corréler dans le cas d'une géométrie fixée et de domaines limités des paramètres opératoires.

EINSETZEN DER STATISCHEN STRÖMUNGSINSTABILITÄT IN EINEM ROHR, EINEM KANAL, EINEM RINGSPALT UND EINEM ROHRBÜNDEL

Zusammenfassung—Ein theoretisches Modell für das Einsetzen der Strömungsinstabilität in einer vertikal aufwärts oder abwärts strömenden Flüssigkeit in einem Kanal mit konstantem Druckverlust wird entwickelt. Das Modell beruht auf den Erhaltungssätzen für Impuls und Energie zusammen mit einer algebraischen Formulierung für den Schlupf der Zweiphasenströmung. Die Ergebnisse der Berechnung werden mit Versuchsdaten bei unterschiedlichen Werten für Druck, Wärmestromdichte, Länge, Eintrittsunterkühlung und Dampfgehalt am Austritt überprüft. Die Vorhersage für die Abhängigkeit des minimalen Massenstroms von diesen Parametern befinden sich in vollständiger Übereinstimmung mit den aus den Versuchsdaten ersichtlichen Tendenzen. Die Daten wurden aus Versuchen an senkrechten Aufwärts- und Abwärtsströmungen in Rohren, Rechteckkanälen, Ringspalten und Rohrbündel-Anordnungen entnommen—und zwar unter den Bedingungen des unterkühlten Siedens wie auch der Netto-Dampfproduktion. Die hier angegebene Datensammlung scheint zu den umfangreichsten, in der Literatur verfügbaren Dateien zu gehören. Die theoretisch ermittelten Ergebnisse legen eine Korrelationsmethode für begrenzte Bereiche der Betriebsparameter bei konstanter Geometrie nahe. Diese Methode wird zusammen mit den spezifischen Korrelationsvorschriften beschrieben.

ВОЗНИКНОВЕНИЕ НЕУСТОЙЧИВОСТИ ТЕЧЕНИЯ В ТРУБАХ, КАНАЛАХ, КОЛЬЦЕВЫХ ЗАЗОРАХ И СТЕРЖНЕВЫХ ПУЧКАХ

Аннотация—Разработана теоретическая модель возникновения неустойчивости течения в канале в случае вертикального восходящего и нисходящего потоков кипящей жидкости с постоянным перепадом давления. Модель основана на уравнениях баланса импульса и энергии с учетом эффектов скорости скольжения в двухфазном потоке. Проведено сравнение теоретических расчетов с экспериментальными данными по давлению, тепловому потоку, длине, недогреву на входе и составу потока на выходе. Теоретические предсказания зависимости минимального массового потока от указанных переменных хорошо согласуются с экспериментальными данными, полученными для случаев вертикального восходящего и нисходящего течений в круглой трубе, прямоугольном канале, кольцевых зазорах и стержневых пучках с учетом парообразования при наличии кипения. Представленная совокупность данных является наиболее полной из имеющихся в литературе. На основе теоретических результатов предложен метод корреляции интервалов режимных параметров для заданной геометрии. Кроме описания метода даны конкретные корреляционные зависимости.